Observations of ozone transport from the free troposphere to the Los Angeles basin

Neuman J. A., M. Trainer, K. A. Aikin, W. M. Angevine, Jérôme Brioude, S. S. Brown, J. A. de Gouw, W. P. Dube, M. Graus, J. H. Flynn, et al.

Observations of ozone transport from the free troposphere to the Los Angeles basin

J. A. Neuman,[1,2] M. Trainer,[2] K. C. Aikin,[1,2] W. M. Angevine,[1,2] J. Brioude,[1,2] S. S. Brown,[2] J. A. de Gouw,[1,2] W. P. Dube,[1,2] J. H. Flynn,[3] M. Graus,[1,2] J. S. Holloway,[1,2] B. L. Lefer,[3] P. Nedelec,[4] J. B. Nowak,[1,2] D. D. Parrish,[2] I. B. Pollack,[1,2] J. M. Roberts,[2] T. B. Ryerson,[2] H. Smit,[5] V. Thouret,[4] and N. L. Wagner[1,2]

Received 22 September 2011; revised 11 January 2012; accepted 13 January 2012; published 9 March 2012.

[1] Analysis of in situ airborne measurements from the CalNex 2010 field experiment (Research at the Nexus of Air Quality and Climate Change) show that ozone in the boundary layer over Southern California was increased by downward mixing of air from the free troposphere (FT). The chemical composition, origin, and transport of air upwind and over Los Angeles, California, were studied using measurements of carbon monoxide (CO), ozone, reactive nitrogen species, and meteorological parameters from the National Oceanic and Atmospheric Administration WP-3D aircraft on 18 research flights in California in May and June 2010. On six flights, multiple vertical profiles from 0.2–3.5 km above ground level were conducted throughout the Los Angeles (LA) basin and over the Pacific Ocean. Gas phase compounds measured in 32 vertical profiles are used to characterize air masses in the FT over the LA basin, with the aim of determining the source of increased ozone observed above the planetary boundary layer (PBL). Four primary air mass influences were observed regularly in the FT between approximately 1 and 3.5 km altitude: upper tropospheric air, long-range transport of emissions, aged regional emissions, and marine air. The first three air mass types accounted for 89% of the FT observations. Ozone averaged 71 ppbv in air influenced by the upper troposphere, 69 ppbv in air containing emissions transported long distances, and 65 ppbv in air with aged regional emissions. Correlations between ozone and CO, and ozone and nitric acid, demonstrate entrainment of ozone from the FT into the LA PBL. Downward transport of ozone-rich air from the FT into the PBL contributes to the ozone burden at the surface in this region and makes compliance with air quality standards challenging.

Citation: Neuman, J. A., et al. (2012), Observations of ozone transport from the free troposphere to the Los Angeles basin, *J. Geophys. Res.*, *117*, D00V09, doi:10.1029/2011JD016919.

1. Introduction

[2] In the troposphere, ozone is a secondary pollutant formed from the reaction of volatile organic compounds (VOCs) and NOx (NOx = NO + NO_2) in the presence of sunlight. Since ground level ozone has deleterious effects on human health and plant growth, ozone and its precursors are regulated. Ozone also has radiative properties that make it an important climate-forcing molecule. The ozone lifetime in the troposphere is increased if ozone and its precursors are lofted above the planetary boundary layer (PBL), where depositional losses on surfaces are reduced. Consequently, after lofting, ozone can be transported long distances or ozone may accumulate above the PBL. Entrainment of this ozone aloft into the PBL affects surface ozone concentrations. Since the 1970s, studies in the LA basin have identified ozone layers aloft that may return to the ground to increase ozone either locally or outside the source region [*Edinger*, 1973; *Blumenthal et al.*, 1978; *McElroy and Smith*, 1993; *Langford et al.*, 2010]. The topographic features of complex terrain can strengthen mixing processes that transport ozone and other species between the free troposphere (FT) and the PBL [*Lu and Turco*, 1996; *Fast et al.*, 2000; *McKendry et al.*, 2001; *Hacker et al.*, 2001]. Downward mixing of free tropospheric ozone, long range transport

[1]Cooperative Institute for Research in Environmental Sciences, University of Colorado Boulder, Boulder, Colorado, USA.
[2]Chemical Sciences Division, Earth System Research Laboratory, NOAA, Boulder, Colorado, USA.
[3]Department of Earth and Atmospheric Sciences, University of Houston, Houston, Texas, USA.
[4]Laboratoire d'Aérologie, Centre National de la Recherche Scientifique, Toulouse, France.
[5]Institute for Chemistry of the Polluted Atmosphere, Research Centre Jülich GmbH, Jülich, Germany.

0148-0227/12/2011JD016919

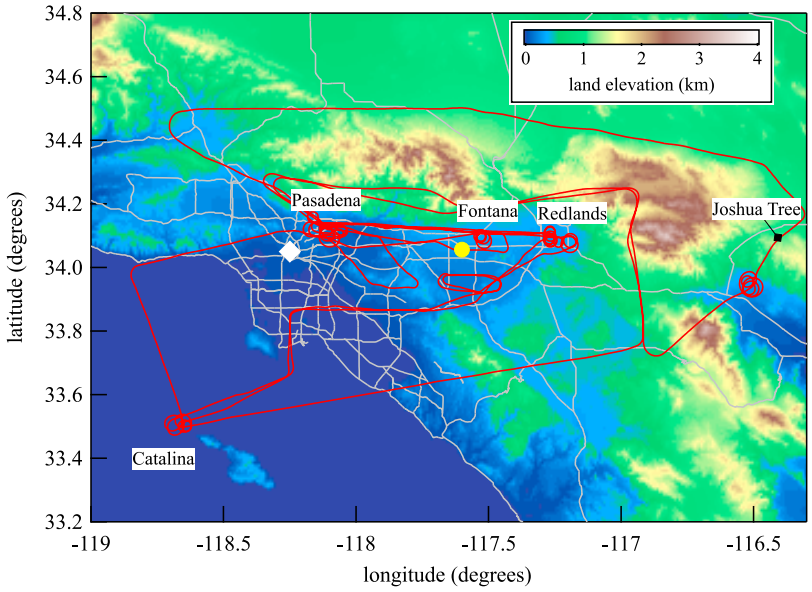

Figure 1. Topographic map of the LA basin, including the location of downtown Los Angeles (white diamond), Ontario (yellow circle), major roads (gray lines), and the WP-3D flight track on 19 May 2010 (red line). Vertical profiles, which are indicated by the flight track spirals, were performed regularly over Catalina, Pasadena, Fontana, and Redlands during CalNex.

of ozone and its precursors, and lofting and subsequent entrainment of regional emissions all have been shown to affect ozone levels along the west coast of the United States (U. S.) [*Parrish et al.*, 2010; *Hudman et al.*, 2004; *Jaffe*, 2011; *Huang et al.*, 2010; *McElroy and Smith*, 1993; *Ambrose et al.*, 2011; *Jacob et al.*, 1999]. Distinguishing locally produced ozone from ozone imported into a region is important for developing effective control strategies.

[3] In the U. S., revisions of the National Ambient Air Quality Standard (NAAQS) for ozone, most recently in 2008, have lowered the exceedance value for compliance with the standard. Currently, attainment of the ozone standard demands that the 3-year average of the annual fourth highest daily maximum 8-h average ozone mixing ratio does not exceed 75 ppbv. Although the 1-s ozone measurements over 75 ppbv in this paper do not represent exceedances, since a violation of the standard occurs only after 8-h average ozone surpasses 75 ppbv multiple times over at least 3 years, they may indicate processes that affect regulatory compliance. The basin that encompasses the entire Los Angeles metropolitan area (LA basin) has a population of 15 million and has suffered high levels of photochemical smog for over a half century [*Haagen-Smit*, 1952]. Many intensive studies have uncovered the dominant processes leading to increased ozone levels in this region [e.g., *Croes and Fujita*, 2003; *Lawson*, 1990]. Although decades of emissions reductions have been effective at mitigating ozone levels, many monitoring locations in the South Coast Air Quality Management District around Los Angeles, CA are still not in attainment of the NAAQS (www.aqmd.gov). Since ozone levels in this region are regularly very near the 75-ppbv exceedance value, small changes in background ozone can appreciably alter the number of exceedances. A global model [*Fiore et al.*, 2002] found that the policy relevant background, which is the ozone level that would exist in the absence of North American emissions [*McDonald-Buller et al.*, 2011], is many tens of ppbv lower than 75 ppbv, such that exceedances can be attributed largely to local and regional emissions. In contrast, other models and measurements along the west coast of the U. S. and in the intermountain west have shown that ozone transported from outside the region can mix to the surface to substantially increase ground level ozone [*Jacob et al.*, 1999; *Parrish et al.*, 2010; *Hudman et al.*, 2004; *Jaffe*, 2011; *Huang et al.*, 2010; *Zhang et al.*, 2011; *Wang et al.*, 2009; *Ambrose et al.*, 2011].

[4] The source of upwind ozone is not always certain, because air reaching the west coast of North America in the spring and summer can be a mixture from many sources without clear chemical signatures that indicate the air mass origin [*Liang et al.*, 2007; *Zhang et al.*, 2008]. Additionally, mixing of regional emissions with upwind air can obscure identification of the origins and fate of ozone. The vertical distribution of gas phase species in the troposphere over Los Angeles and the adjacent Pacific Ocean are studied here using a comprehensive set of in situ chemical measurements. In this study, air masses in the free troposphere (FT) over the LA basin are categorized by their distinctive chemical characteristics that enable identification of the origin of ozone aloft. Free tropospheric air with increased ozone is demonstrated to mix into the PBL and increase ozone levels at the surface.

2. Experiment

2.1. Study Region

[5] The South Coast Air Basin (www.arb.ca.gov/adam/netrpt/) encompasses Los Angeles, CA and the land basin between the Pacific Ocean and the surrounding mountains shown in Figure 1. Vehicle emissions are large throughout the basin, especially near the dense network of roads around downtown Los Angeles (Figure 1). The mountains that surround the LA basin strongly influence the distribution of

trace gases in the region. The San Gabriel Mountains north of Fontana rise to 3.1 km, and the San Bernardino Mountains east of Redlands reach 3.5 km. During the midday, westerly winds often carry air to the eastern end of the basin (in the vicinity of Redlands), where emissions can be trapped, lifted by mountains, or transported through mountain passes.

2.2. WP-3D Aircraft Flights

[6] The instrumented National Oceanic and Atmospheric Administration (NOAA) WP-3D aircraft flew 18 research flights from Ontario, CA between 4 May and 20 June 2010 during the CalNex 2010 experiment (Research at the Nexus of Air Quality and Climate Change, http://www.esrl.noaa.gov/csd/calnex/). The maximum flight altitude was 6.7 km, and the greatest flight duration was 7.7 h. This paper uses data primarily from seven daytime flights that focused on the LA Basin. The flight track on 19 May shown in Figure 1 illustrates the sampling strategy, with measurements upwind along the Pacific Coast and downwind over receptor regions inland from Los Angeles. Extensive sampling was conducted in the eastern part of the LA Basin where emissions and photochemically processed secondary pollutants accumulated. The other daytime flights in the LA basin on 4, 8, 14, 16, and 21 May and 20 June 2010 followed similar flight tracks, and included multiple vertical profiles on both weekends and weekdays. Several flight segments conducted over the southern San Joaquin Valley and over the high desert east of Los Angeles are also examined.

[7] Vertical profiles at several locations are used to characterize the air that enters and exits the LA Basin. Spiral altitude profiles were performed regularly over four locations on six of the seven daytime flights in the LA Basin. Between 4–9 profiles were performed on each flight, with a total of ten over Catalina Island, seven over Pasadena, six over Fontana, and nine over Redlands (Figure 1). In total, over 27,000 1-s observations of many molecules and meteorological parameters were obtained in 32 profiles. The profiles were performed between 11 A.M. and 4:30 P.M. Pacific Daylight Time (PDT), with most measurements obtained in the mid-afternoon. Most profiles were ascending or descending spirals with approximately 10 km radii from 0.2–3.5 km above ground level (AGL). Near Catalina Island, a few profiles descended as low as 0.1 km above sea level (ASL). The surface elevations of Redlands and Fontana are approximately 0.47 km ASL and that of Pasadena is 0.28 km ASL. A few spirals ascended and descended over the same location, and some included steps, where the aircraft maintained a constant altitude for approximately 5 min before ascending or descending to the next level.

2.3. Measurements

[8] In situ trace gas measurements used for this analysis include both primary emissions and secondary oxidation products. One-second average measurements are analyzed here, so that the spatial resolution for the aircraft traveling at a nominal 100 m/s airspeed was 0.1 km. The aircraft ascent and descent rates ranged from 5–10 m/s, so that 1-s measurements yielded a vertical resolution of at least 10 m. Measurements of carbon monoxide (CO), NOx, peroxyacetic nitric anhydride (PAN, $CH_3C(O)O_2NO_2$), nitric acid (HNO_3), and water vapor are used to identify the origin of transported ozone. CO is directly emitted and has a long (months) atmospheric lifetime, and thus is useful for identifying fresh emissions and those transported from afar. NOx is also directly emitted, but its lifetime is on the order of hours to days. Consequently, NOx is useful for distinguishing the age of pollution from local sources. HNO_3 is formed in the atmosphere from NOx oxidation and has a lifetime affected by wet and dry deposition. HNO_3 levels are usually small in fresh emissions, the upper troposphere (UT) [*Neuman et al.*, 2001], and in emissions transported long distances [*Nowak et al.*, 2004]. Increased HNO_3 levels indicate influence from either the stratosphere or aged regional emissions. Water vapor abundance in the FT over the LA basin distinguishes air masses influenced by the dry UT from those containing air from the more humid PBL.

[9] CO was measured once per second by a vacuum ultraviolet fluorescence instrument with 5% uncertainty and 1 ppbv precision [*Holloway et al.*, 2000]. HNO_3 was measured once per second by chemical ionization mass spectrometry (CIMS) using SiF_5^- as the reagent ion [*Neuman et al.*, 2002]. Compared to previous aircraft studies with the same instrument, the sensitivity improved from 1 ion count per second per pptv HNO_3 (Hz/pptv) to 2.5 Hz/pptv, and the instrumental background was reduced. A newly constructed heated Teflon inlet reduced interaction of the sampled air with inlet surfaces [*Neuman et al.*, 1999] to decrease measurement uncertainty and improve detection limits. HNO_3 was measured without interference from particulate nitrate [*Neuman et al.*, 2003a]. Instrument uncertainty, determined from in-flight calibrations [*Neuman et al.*, 2003b] and background determinations, was $\pm$ (15% + 0.040 ppbv), and the 1σ precision was 0.012 ppbv for the 1-s measurements. Ammonia (NH_3) was measured once per second by CIMS [*Nowak et al.*, 2007]. Measurement uncertainty differed for each flight, with typical uncertainties of $\pm$ (30% + 0.2 ppbv) and a 1σ precision of 0.08 ppbv for the 1-s measurements. PAN was measured once every 2 s by CIMS [*Slusher et al.*, 2004], with an uncertainty of $\pm$ (20% + 0.005 ppbv).

[10] Two independent instruments measured ozone, NO, and NO_2: a chemiluminescence detector (CLD) and a cavity ring-down spectrometer. Ozone measured by NO-induced chemiluminescence [*Ryerson et al.*, 1998] had an uncertainty of $\pm$ (2% + 0.015 ppbv), and NO measured by ozone induced chemiluminescence had an uncertainty of $\pm$ (3% + 0.01 ppbv). NO_2 concentrations were determined with $\pm$ (4% + 0.03 ppbv) uncertainty [*Pollack et al.*, 2011] by photolyzing atmospheric NO_2 to NO using a UV-LED converter, followed by ozone-induced chemiluminescence of NO. Improvements to instrument hardware, calibration, and operation reduced the NO, NO_2, and ozone uncertainties compared to previously reported WP-3D nitrogen oxides and ozone data [e.g., *Neuman et al.*, 2009]. Data from the CLD were used for most of the analysis, since the CLD measured NOx and ozone with greater precision than the cavity ring-down spectrometer (5% uncertainty [*Wagner et al.*, 2011]). When the CLD was not operational on the 14 May flight and during instrument calibration periods on other flights, data from the cavity ring-down spectrometer were used. In the results that follow, titration of ozone to NO_2 by NO when NOx mixing ratios were large is accounted for by using odd

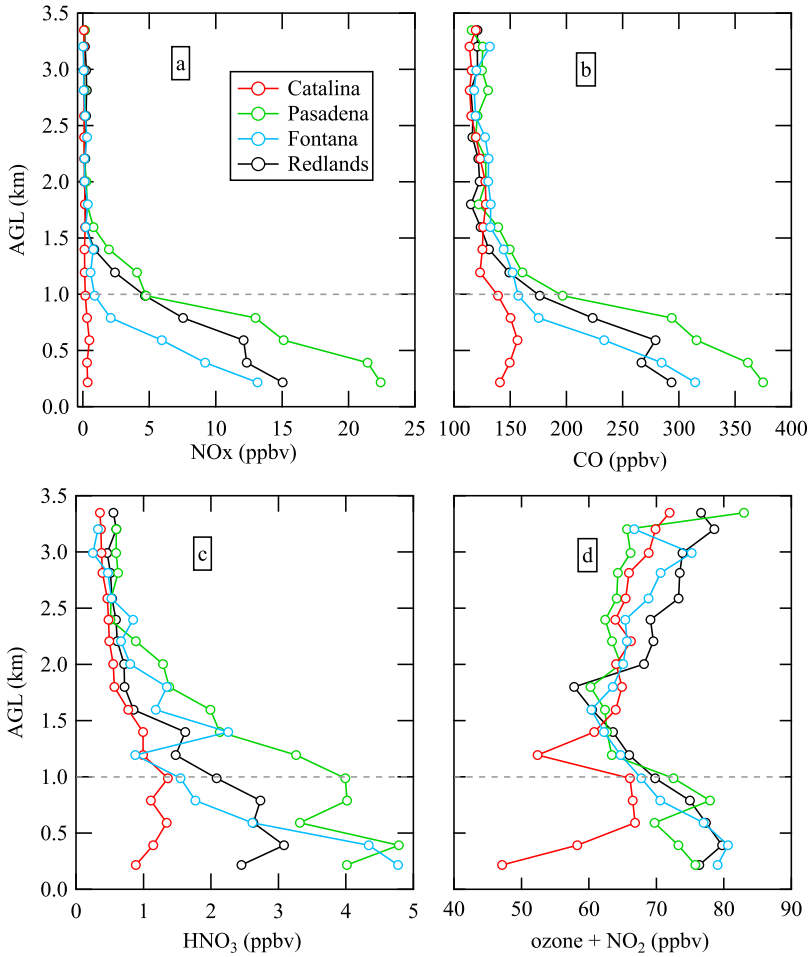

Figure 2. Average (a) NOx, (b) CO, (c) HNO_3, and (d) ozone+NO_2 vertical profiles over Catalina (red), Pasadena (green), Fontana (blue), and Redlands (black). Each point is an average over 0.2 km altitude of approximately 400 1-s measurements from 6–10 vertical profiles. The gray dashed line indicates the average boundary layer height at the three inland locations.

oxygen (Ox = NO_2 + O_3) in the analysis. Above the PBL, ozone and Ox differed by less than 1%, since ozone levels were over 100 times larger than NO_2 in the FT measured here. For simplicity, ozone rather than Ox is used when discussing air in the FT and outside the LA Basin, where NO_2 was negligible compared to ozone.

3. Results

3.1. Average Vertical Distribution of Trace Gases

[11] The average vertical distributions of trace gases reveal several important characteristics of the Los Angeles emissions and air upwind and over the LA basin. NOx, CO, HNO_3, and Ox measured in 32 vertical profiles over Catalina, Pasadena, Fontana, and Redlands are averaged into 0.2 km altitude bins (Figure 2). During these midday flights, the PBL height, determined from aircraft measurements of potential temperature, ranged from 0.6–1.8 km AGL and averaged 1.0 ± 0.3 km AGL at the three inland locations. Differences in the PBL chemical composition reflect the proximity to sources at each location. CO, ozone, and reactive nitrogen in the boundary layer near Catalina Island, which is over 50 km west of the coast and usually upwind of large emissions from Los Angeles, were considerably lower than at the inland locations. CO and NOx were greatest over Pasadena, which is closest to and downwind from high emissions from Los Angeles. Boundary layer Ox was greatest farthest downwind from Los Angeles at Fontana and Redlands, where the air was the most photochemically processed. HNO_3 was lower at Redlands than at Fontana or Pasadena, as a consequence of reaction with large NH_3 mixing ratios (J. B. Nowak et al., Ammonia sources in the California South Coast Air Basin and their impact on ammonium nitrate formation, submitted to *Geophysical Research Letters*, 2012) that caused conversion of gas phase HNO_3 to particulate nitrate [*Neuman et al.*, 2003a]. In altitude profiles above Redlands, NH_3 exceeded 50 ppbv in the PBL on four of the flights studied here, and was as high as 350 ppbv. At the other locations NH_3 was usually less than 10 ppbv and never exceeded 18 ppbv.

[12] Measurements of short-lived species in the FT above the LA Basin are used to identify rapid vertical transport from the LA Basin PBL to the FT. At the inland locations (Pasadena, Fontana, and Redlands), NOx in the PBL was approximately 2 orders of magnitude greater than in the FT. The NOx observations demonstrate that fresh emissions

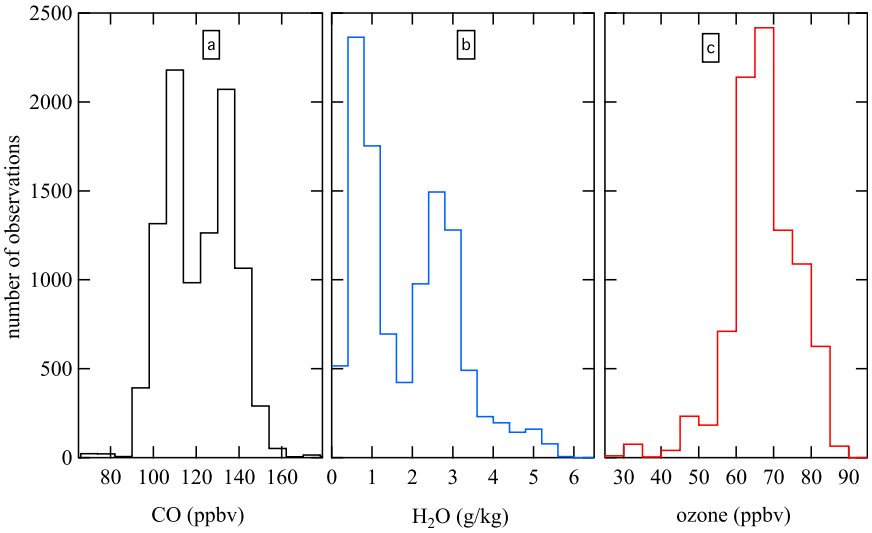

Figure 3. Histogram of 1-s measurements of (a) CO, (b) water vapor and (c) ozone in the FT between 1.8–3.5 km AGL from 32 vertical profiles over the LA Basin. The CO and water vapor measurements are used to determine four air mass classifications, as described in section 3.2.

were not rapidly vented to the FT. The contrast between the FT and PBL for the secondary species HNO_3 and ozone was much less sharp.

[13] In the FT, the trace gas vertical distributions were similar above all four locations. Nearly 8800 1-s measurements of each molecule were acquired on six flights above the PBL between 1.8–3.5 km. NOx mixing ratios showed little altitude variation and were consistently small. Averaging all 1-s measurements above 1.8 km AGL from the 32 vertical profiles gives NOx = 0.13 ± 0.2 ppbv and PAN = 0.19 ± 0.1 ppbv. CO also varied little with altitude in the FT, with mixing ratios that clustered around two values (discussed in section 3.2.). In contrast, HNO_3 and ozone varied substantially with altitude. HNO_3 mixing ratios decreased slowly with altitude in the FT. The same altitude dependence was apparent in both ascending and descending profiles, and also in step profiles that dwelled at several constant altitude levels for minutes. The consistency of this finding demonstrates that atmospheric processes, and not instrumental artifacts, give rise to the HNO_3 vertical distribution. Since HNO_3 is usually decreased in the UT [*Neuman et al.*, 2001], marine air, and trans-Pacific transport of emission plumes from Asia [*Nowak et al.*, 2004] and increased in aged urban plumes [e.g., *Neuman et al.*, 2002], increased HNO_3 provides a sensitive marker for transport of aged regional emissions to the FT. Ozone exhibited an entirely different altitude profile, with frequent large enhancements aloft. Since the FT above the LA basin was horizontally homogeneous for each trace gas, a few general air mass classifications may be used to describe this entire region of the atmosphere.

3.2. Free Tropospheric Air Mass Classifications

[14] Air masses in the FT over the LA basin are categorized by their chemical composition with the goal of identifying the transport pathways of air masses into this region, and thereby determining the source of ozone above the PBL. Sources that may contribute to the composition of the FT over the LA basin include marine boundary layer air, aged regional emissions from the southern California PBL, long-range transport of emissions, the UT, and the stratosphere. Water vapor and CO provide clear indications of air mass history. Large water vapor mixing ratios in the FT indicates an influence from marine or continental air, while small water vapor mixing ratios are present in air masses that descended from the UT or stratosphere. Increased CO reveals an influence from emissions lofted from the region or transported long distances, and background levels of CO are characteristic of stratospheric, UT, or marine influences. Emissions from Asia [e.g., *Hudman et al.*, 2004; *Jacob et al.*, 1999] and Canada and Mexico [*Wang et al.*, 2009] can be transported to southern California.

[15] Air masses are categorized by measured CO and water vapor mixing ratios in the FT between 1.8–3.5 km. Measurements above 1.8 km AGL (the highest boundary layer observed over Los Angeles here) are used to classify the FT in order to discriminate against any observations from the PBL. CO clustered around two values (110 ppbv and 135 ppbv, Figure 3a) that clearly separated air influenced by emissions (CO > 120 ppbv) from marine, UT or stratospheric air (CO < 120 ppbv). Coincidentally, CO levels were similar in air influenced by aged regional emissions and long-range transport of emissions. Water vapor mixing ratios also clustered around two values that distinguished dry air that descended from higher altitudes (H_2O < 2 g/kg, Figure 3b) from wetter air that was lofted from the PBL (H_2O > 2 g/kg, Figure 3b). Wetter air was observed in the FT on the flights of 14, 16, and 19 May. On 4 and 8 May and 20 June, the air in the FT was considerably drier. Increased CO mixing ratios were observed in both wet and dry air masses. Since both water vapor and CO clustered around two values as shown in Figure 3, four air mass classifications determined by CO and water vapor mixing ratios are sufficient to include all the FT observations here. Air in the FT over the LA basin is classified as marine influenced when CO < 120 ppbv and H_2O > 2 g/kg. When CO > 120 ppbv and H_2O > 2 g/kg,

Table 1. Free Tropospheric Air Mass (FT Air Mass) Chemical Characteristics in the Four Air Mass Types Determined in Section 3.2[a]

FT Air Mass	Dates (2010)	Water Vapor (g/kg)	CO (ppbv)	HNO_3 (ppbv)	PAN (ppbv)	Ozone (ppbv)	Fraction of Observations (%)
UT	4 May, 8 May	0.8 ± 0.4	108 ± 6	0.4 ± 0.1	0.11 ± 0.04	71 ± 8	38
Long range transport	8 May, 20 June	1.0 ± 0.4	136 ± 10	0.2 ± 0.2	0.21 ± 0.09	69 ± 6	16
Aged regional emissions	14, 16, 19 May	3.0 ± 0.6	134 ± 7	0.9 ± 0.5	0.27 ± 0.13	65 ± 4	34
Marine	19 May	3.4 ± 1	106 ± 10	0.8 ± 0.4	0.15 ± 0.08	53 ± 10	11

[a]For each air mass classification, the dates and average water vapor, CO, HNO_3, PAN, ozone, and fraction of observations measured in vertical profiles between 1.8–3.5 km over the LA basin are shown.

the air was influenced by aged regional emissions. Air masses affected by long range transport of emissions had CO > 120 ppbv and H_2O < 2 g/kg. A UT influence was prominent when CO < 120 ppbv and H_2O < 2 g/kg.

[16] Reactive nitrogen partitioning provides additional indications of air mass sources. Reactive nitrogen partitioning often favors PAN over HNO_3 in emission plumes transported long distances [*Nowak et al.*, 2004; *Roberts et al.*, 2004]. Both HNO_3 and PAN are significantly enhanced in aged regional emissions, and both are minimal in the UT that has not seen recent (several days) contributions from urban emissions or stratospheric intrusions. Stratospheric intrusions are distinguished from UT air by the relationship between HNO_3 and ozone. HNO_3 is decreased in the UT and has a source in the stratosphere, where HNO_3 is highly correlated with ozone [*Popp et al.*, 2009]. The UT air with CO < 120 ppbv and H_2O < 2 g/kg measured here was not recently influenced by the stratosphere, since HNO_3 was small and uncorrelated with ozone. Although ozone in the FT was not from recent stratospheric intrusions, the stratosphere may still have contributed to the ozone levels in the UT by much slower mixing over extremely long paths [*Trickl et al.*, 2011]. Although recent stratospheric intrusions were not observed below 4 km on the six flights studied here, they were observed over California on other days [*Langford et al.*, 2012] and from the WP-3D at higher altitudes. For example, on 11 May at 4.5–5.5 altitude over the southern San Joaquin Valley, ozone reached 180 ppbv in air with CO < 120 ppbv, H_2O < 2 g/kg, and HNO_3 was positively correlated with ozone (slope = 0.007, r^2 = 0.91).

[17] The four air mass classifications for the FT from 1.8–3.5 km and the corresponding CO, water vapor, reactive nitrogen, and ozone levels are given in Table 1. These classifications also describe the FT between the top of the PBL (which averaged 1 km AGL) up to 1.8 km for each vertical profile. Ozone levels in the different air mass types are discussed in section 4.1.

3.3. Vertical Profile Examples

[18] Individual vertical profiles illustrate the free tropospheric air mass types that were observed and reveal some characteristics of the transport responsible for the trace gas mixing ratios above LA. Three profiles that represent different meteorological conditions and trace gas vertical distributions are shown in Figures 4, 5 and 6. UT air was sampled above the PBL on a spiral ascent from 0.3–2.8 km over Redlands at 3:20 P.M. PDT on 8 May 2010 (Figure 4). The PBL height, indicated by a sharp change in potential temperature, was 1.8 km AGL. The winds were predominately from the west, with speeds of 7–13 m/s in the FT and

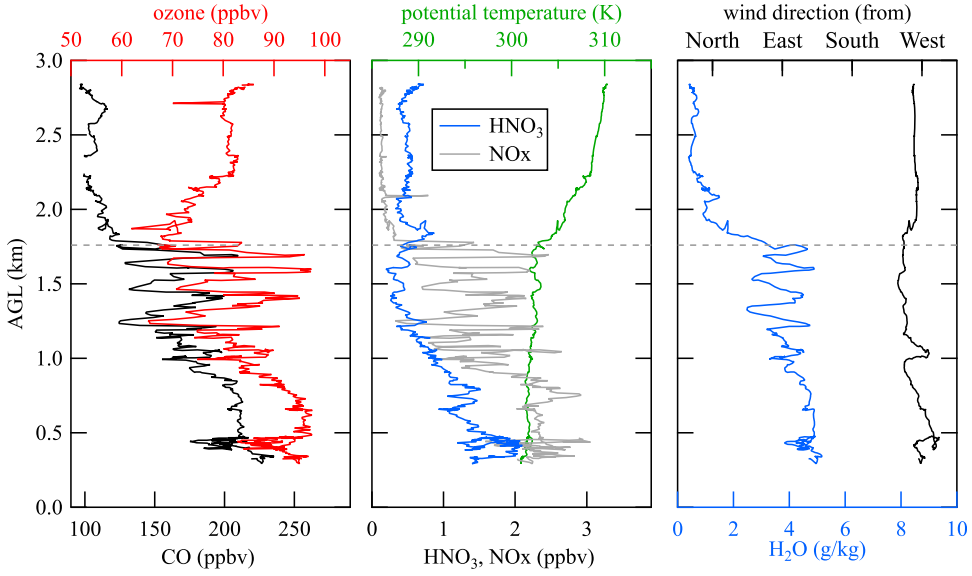

Figure 4. One-second ozone (red), CO (black), HNO_3 (blue), and NOx (gray) measurements and meteorological observations (potential temperature in green, wind direction in black, and water vapor in blue) during a spiral ascent over Redlands, CA at 3:20 P.M. PDT on 8 May 2010. The gray dashed line indicates the boundary layer height.

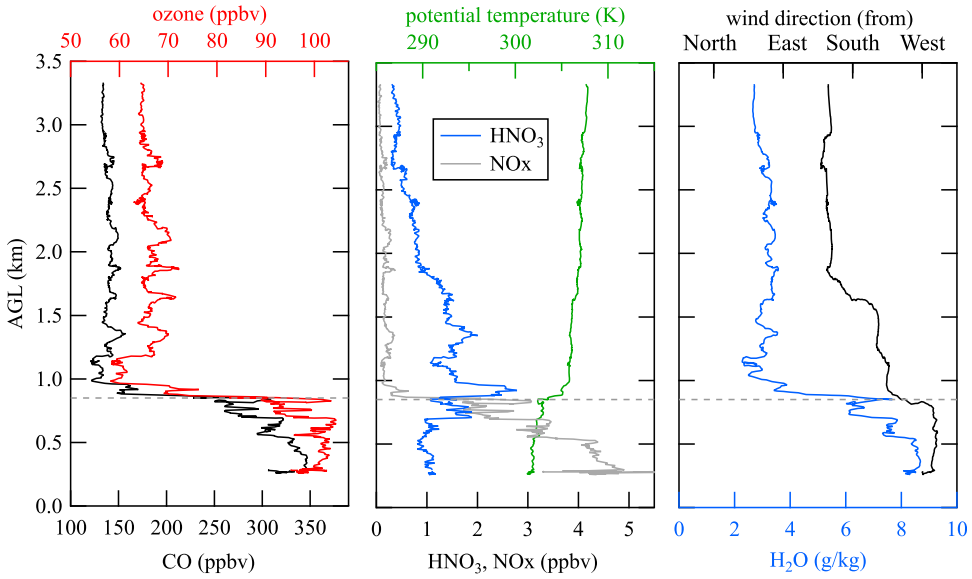

Figure 5. Same as Figure 4 but for a spiral ascent at 2:55 P.M. PDT on 16 May 2010.

1–4 m/s in the PBL. Within the PBL over Redlands, CO exceeded 200 ppbv and ozone was over 95 ppbv. The large variability above 1 km in the PBL likely was caused by small scale turbulence associated with vertical transport, similar to that reported from remote ground sites [*Parrish et al.*, 1998]. In the FT, the air was considerably cleaner and drier, with reduced CO (104 ± 5 ppbv), NOx (0.14 ± 0.06 ppbv), and water vapor (0.7 ± 0.3 g/kg). Ozone, however, increased with altitude in the FT and was uncorrelated with the other trace gases above 1.8 km. Increased ozone, and decreased water vapor, CO, HNO_3, and NOx in the FT are interpreted as an air mass influenced by transport from the UT without recent influence from long-range transport of emissions or the stratosphere. These features were repeatedly observed on 4 and 8 May.

[19] On three flights, aged regional emissions were encountered above the PBL. Wet air masses with increased CO and HNO_3 were observed in the FT on 14, 16, and 19 May. For example, in the FT above 1 km over Redlands on 16 May (Figure 5), the winds were predominately from the SE at 3–7 m/s, and the air was humid compared to 8 May. Additionally, ozone varied little with altitude and was positively correlated with CO. Although NOx (0.15 ± 0.06 ppbv above 1 km) was as small as on 8 May, HNO_3 was nearly ten times greater. The increased HNO_3 and water vapor, minimal NOx, positive correlation between CO and ozone, and winds from the southeast indicate aged regional emissions in the FT above Los Angeles. Three vertical profiles on 19 May (not shown) had increased water vapor but small amounts of reactive nitrogen and CO in the FT, suggesting a marine influence.

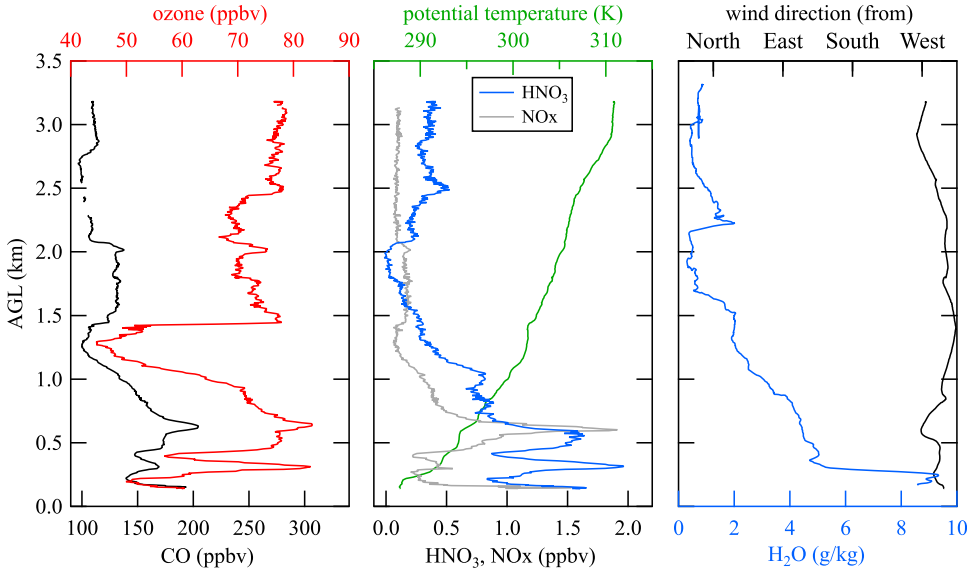

Figure 6. Same as Figure 4 but for a profile near Catalina Island at 12:15 P.M. PDT on 8 May 2010.

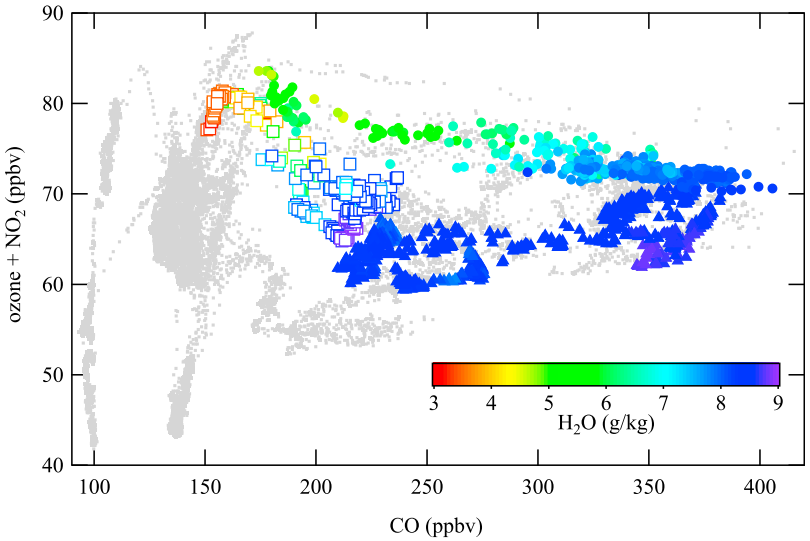

Figure 7. One-second measurements of ozone+NO_2 versus CO from the WP-3D flight on 14 May 2010 (gray dots). Measurements acquired during a mid-afternoon flight segment over the eastern LA basin are colored by water vapor mixing ratio, with different symbols that indicate aircraft location. The WP-3D flew from Chino past Riverside at 0.8 km AGL (open squares), then to Pasadena between 0.8 and 0.3 km AGL (solid circles), and finally southeast from Pasadena past Fullerton at 0.3 km AGL (solid triangles).

[20] On occasion, more than one air mass type was encountered in a single vertical profile, and vertical layers with distinct chemical composition were observed in the FT over the LA basin. For example, above Catalina Island on 8 May, the vertical distribution of trace gases consisted of several discrete layers (Figure 6). Between 1.5–2.0 km, CO mixing ratios were more than 30 ppbv larger than in the air a couple hundred meters above or below. In this layer, decreased water (H_2O < 1 g/kg) and HNO_3 near zero indicates that precipitation dehydrated the air mass and removed HNO_3 by wet deposition. PAN was increased (0.29 ± 0.05 ppbv, not shown) and the ratio of CO to reactive nitrogen was much larger than measured in the PBL, as a consequence of reactive nitrogen removal. The increased CO and PAN and decreased water vapor and HNO_3 indicate influence from the long-range transport of emissions. Between 2.5–3 km, ozone and water vapor were similar to the layer below, but PAN and CO were reduced and HNO_3 was increased. This layer was more characteristic of the UT (Figure 4), and the positive correlation between HNO_3 and ozone suggests some contribution from stratospheric air as well. Although ozone was approximately 75 ppbv in both layers, differences in air mass chemical composition demonstrate that the ozone sources and transport processes were not the same. Air masses influenced by long-range transport of emissions also were observed on the 20 June vertical profiles.

3.4. Mixing Deduced From Correlations

[21] Relationships between ozone and other trace gases, which have long been used to identify and quantify photochemical ozone production [e.g., *Trainer et al.*, 1993; *Chin et al.*, 1994], also are valuable for determining air mass sources. In transported air masses, positive correlation between ozone and CO is a signature of photochemical ozone production from anthropogenic precursors, and increases in ozone with little change or decreases in CO indicates vertical ozone transport from the FT or stratosphere [*Parrish et al.*, 1998]. Differing Ox to CO relationships, determined from correlation slopes of linear least squares fits, are examined here to indicate the sources of ozone to the LA basin PBL.

[22] The relationships of ozone with CO on the 14 May 2010 flight (Figure 7) show that air from the FT influenced the atmospheric composition in the LA basin PBL. The flight was conducted over the LA basin and upwind of LA over the Pacific Ocean from 10 A.M.–4 P.M. PDT, with a maximum altitude of 3.5 km. The PBL height on this flight, determined from aircraft vertical profiles over Pasadena, Fontana, and Redlands, ranged from 0.6 to 0.8 km AGL. With the exception of a few concentrated ship plumes, NOx was less than 0.5 ppbv, and Ox and ozone were nearly equivalent over the Pacific. All 1-s measurements of Ox and CO are shown in Figure 7 (gray dots), and a 30-min flight segment at low altitude (0.2–0.8 km AGL) in the mid afternoon over the eastern LA basin is colored by water vapor. Ozone varied from 40 ppbv at the lowest altitudes (below 0.4 km in the marine boundary layer) to 80 ppbv above 3 km altitude. The colored points were measured in the well-mixed PBL, or at the top of the PBL. The mixing of three different air masses caused three distinct Ox to CO correlation slopes. CO emissions and photochemically processed ozone precursors mixed with clean marine air during transport across the LA basin and caused increased water vapor and a positive correlation between Ox and CO (solid triangles in Figure 7). Dry air with increased ozone and decreased CO (red and yellow squares in Figure 7) also had little HNO_3 and NOx (not shown), and was compositionally similar to the UT air shown in Figure 4. Vertical mixing of

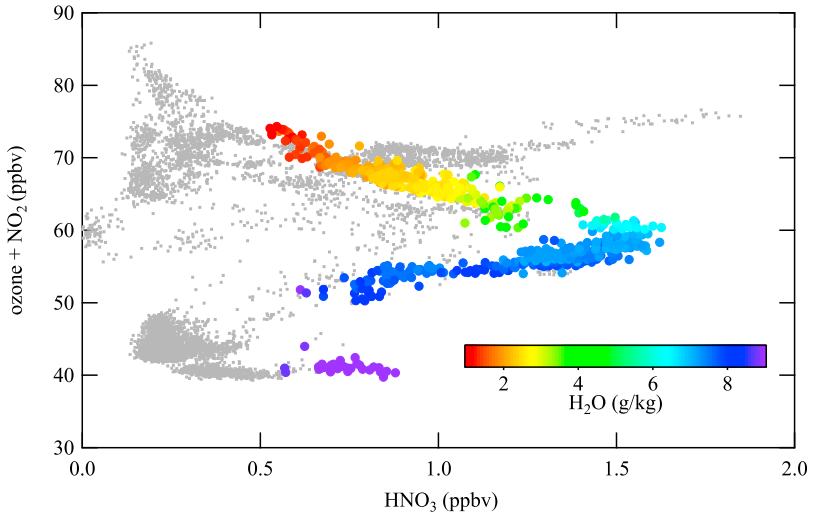

Figure 8. One-second measurements of ozone+NO_2 versus HNO_3 on 21 May 2010 (gray dots), when the WP-3D flew over the ocean west of Los Angeles. The colored points are from the takeoff and subsequent transit over the LA basin at 1 km altitude, when the aircraft flew west over Pasadena and Santa Monica on the way to the Pacific Ocean. In the dry air mass (water vapor mixing ratios <3 g/kg), winds were from the NW at 4–14 m/s.

this dry air from the FT with air in the LA basin caused a negative Ox to CO correlation slope. Two mixing lines with differing negative slopes arise because the FT air mixed into two types of PBL air: marine influenced air with decreased CO (open squares in Figure 7) and urban air with increased CO (solid circles in Figure 7). The negative Ox to CO correlation (colored circles in Figure 7) demonstrates that air from the FT that mixes into the PBL over the LA basin can cause an approximately 20 ppbv ozone increase in the PBL without a corresponding increase in CO.

[23] The relationships between ozone and the products of NOx oxidation also indicate that vertical mixing was a source of ozone to the PBL over the LA basin. At both rural and urban sites, positive correlation between ozone and the products of NOx oxidation is a signature of ozone production from anthropogenic NOx emissions [*Trainer et al.*, 1993]. Since HNO_3 is a NOx oxidation product, a positive correlation between Ox and HNO_3 can represent an anthropogenic influence. A negative or flat correlation between Ox and HNO_3 can be caused by UT air with more ozone and less HNO_3 mixing with boundary layer with increased ozone and HNO_3.

[24] The relationships of ozone with HNO_3 on the 21 May flight over the LA Basin and Pacific Ocean (Figure 8) shows that FT air mixed into the LA basin PBL. The 8:30 A.M. PDT takeoff was followed by a westward transit at 1 km altitude (colored points in Figure 8) over the LA basin from Ontario to Pasadena to the coast near Santa Monica. Early in this flight segment, the water vapor mixing ratio was large and there was a positive correlation between Ox and HNO_3. Above the PBL (0.63 km deep near Ontario at 8:30 A.M. PDT), water vapor and HNO_3 were decreased, and Ox was increased. The chemical composition of this dry air mass with minimal HNO_3 and increased Ox reveal its UT origins. When HNO_3 was approximately 0.6 ppbv, ozone was 20 ppbv higher in the dry air with UT influences compared to the wet air with boundary layer characteristics. Three hours later, the boundary layer over Ontario had grown to 1.2 km, and the dry air with increased ozone aloft was entrained. The negative correlation between Ox and HNO_3 illustrates that FT air mixed into the LA basin.

4. Discussion

4.1. Free Tropospheric Ozone Mixing Ratios

[25] The four air mass classifications (Table 1) inferred from the chemical composition indicate the sources of ozone to the FT. In the FT between 1.8–3.5 km, ozone ranged from 27–88 ppbv and averaged 67 ± 9 ppbv. The UT air mass classification had the greatest ozone (71 ± 8 ppbv) and accounted for 38% of the air masses sampled in vertical profiles between 1.8–3.5 km. Air influenced by long-range transport of emissions had similar ozone levels in the FT (69 ± 6 ppbv), and accounted for 16% of the vertical profiles. Concentrated plumes from Asia, like those previously observed over the Eastern Pacific Ocean (CO = 198 ± 40 ppbv in the work of *Nowak et al.* [2004]) were never observed in the FT here. Instead, CO in transported plumes (CO = 136 ± 10 ppbv, Table 1) was highly diluted, consistent with transpacific transport of Asian emissions that affect air quality in the western U.S. by increasing background levels, rather than by causing large increases in pollutants confined to episodic Asian plumes [*Zhang et al.*, 2008]. Wet air containing aged regional emissions was observed regularly (34% of the vertical profile observations in the FT). Ozone was slightly lower in these air masses, averaging 65 ± 4 ppbv. Ozone averaged 53 ± 10 ppbv in the 11% of FT observations with marine characteristics.

[26] In the FT above the LA basin, ozone averaged over 65 ppbv in three air mass types that accounted for 89% of the sampled air masses. The greatest ozone levels in the FT just above the LA basin PBL were in dry air that likely descended from the UT. The FT ozone levels observed here

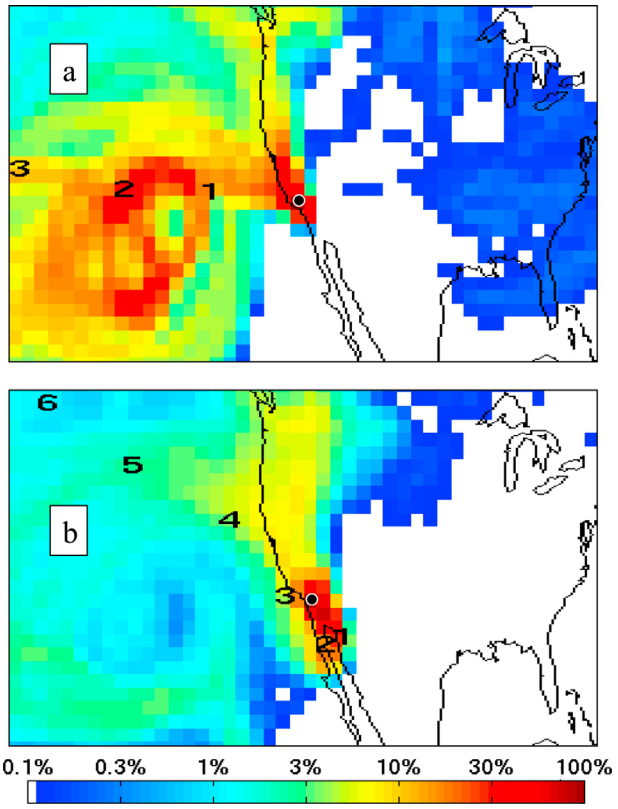

Figure 9. Air mass histories for measurements in the free troposphere at 2 km altitude over Redlands (black circle) on (a) 8 May and (b) 16 May, as determined by the Flexpart Lagrangian particle dispersion model using ERA-interim meteorological fields. The total column residence time in each 1° × 2° grid cell is colored as a percentage of the greatest residence time in a grid cell using a logarithmic scale. The numbers on the maps of North America represent the position of the center of mass of the retroplume at the number of days backward from the position of the measurements.

(Figure 3c) are significant, since they are comparable to the 75 ppbv NAAQS exceedance value. Although dilution, which is not quantified here, reduces the effects of downward mixing of FT ozone to the surface, mixing of FT air into the PBL as shown in section 3.4 may increase ozone to levels that could cause an exceedance. Further, recent evidence points to increasing ozone in the North Pacific troposphere [*Parrish et al.*, 2004] and the springtime middle and upper troposphere over North America [*Cooper et al.*, 2010], so influence of upwind and overhead ozone may grow in importance and challenge the ability of local controls to reduce ozone sufficiently to comply with the U.S. standard.

4.2. Backward Trajectories

[27] Backward trajectories further elucidate the source of air upwind and over the LA basin [*Cooper et al.*, 2011]. The FLEXPART Lagrangian particle dispersion model determined air mass histories by simulating the transport of the air mass backward in time from points along the aircraft flight track [*Stohl et al.*, 2005]. These backward trajectories were performed using three different simulated meteorological fields. Regional-scale air mass histories for three days preceding the observations were calculated using the Weather Research and Forecasting (WRF) model with a 4 × 4 km output resolution. Global scale histories were determined for the preceding 20 days with a 1° × 2° output resolution using both the 3-hourly NCEP Global Forecast System with 0.5° × 0.5° resolution (GFS), and the 6-hourly European Centre for Medium-Range Weather Forecasts interim Reanalysis (ERA-interim) model [*Simmons et al.*, 2007] with approximately 0.7° × 0.7° resolution.

[28] The FLEXPART air mass histories are qualitatively consistent with the observed chemical composition in each vertical profile. Using the chemical composition observations, air masses in the FT were classified as having primarily UT or long-range transport influences on 4 and 8 May and 20 June (Table 1). Winds were from the west and HNO_3 was minimal, showing that air in the FT was not in recent contact with the North American continent. Consistent with the observations, backward trajectories show that air in the FT over the LA basin on 4 and 8 May and 20 June came from the west and had resided over the Pacific Ocean west of California and Mexico the prior week. As an example, Figure 9a shows the Flexpart retroplume (air mass history) from 2 km altitude over Redlands on 8 May, when the FT was influenced by the UT as shown in Figure 4. In contrast, on 14, 16, and 19 May, the chemical composition of air masses in the FT over the LA basin revealed recent boundary layer influence. Observed winds were southeasterly, and CO and water vapor were increased in the FT. Backward trajectories showed that air transported to the aircraft location in the FT remained over the LA basin and the continental U.S. the previous three days. Figure 9b shows the Flexpart retroplume from 2 km altitude over Redlands on 16 May, when the FT was influenced by aged regional emissions as shown in Figure 5. This modeled recirculation of air over the LA basin is consistent with the observed boundary layer influences upon the FT. Since the air in the FT over the LA basin stagnated for several days, compounds from the PBL could accumulate in the FT by slow injection from the PBL.

[29] However, quantitative comparisons of measured and modeled trace gas mixing ratios in the LA basin showed large differences. The FLEXPART model also determined the CO contribution from surface sources, so that measured and modeled CO can be compared. The terrain features of the LA basin and temporal variations in winds cause large variability in CO that is challenging to accurately model. Terrain-driven circulation [e.g., *Lu and Turco*, 1996] demands high spatial resolution, and diurnal changes in low-level winds caused by the land-sea breeze effect require that winds be modeled with high temporal resolution. Although the FLEXPART model showed wind directions that corresponded to the observations, the spatial and vertical distribution of CO was not replicated. For example, large observed CO enhancements at Redlands caused by advection from high emission regions were hundreds of ppbv greater than modeled by FLEXPART. And CO in the FT was consistently too large in the lower resolution GFS and ERA-interim driven model runs, and too small in the higher resolution WRF model runs. Uncertainties in emissions inventories further weaken the connection between measurement and

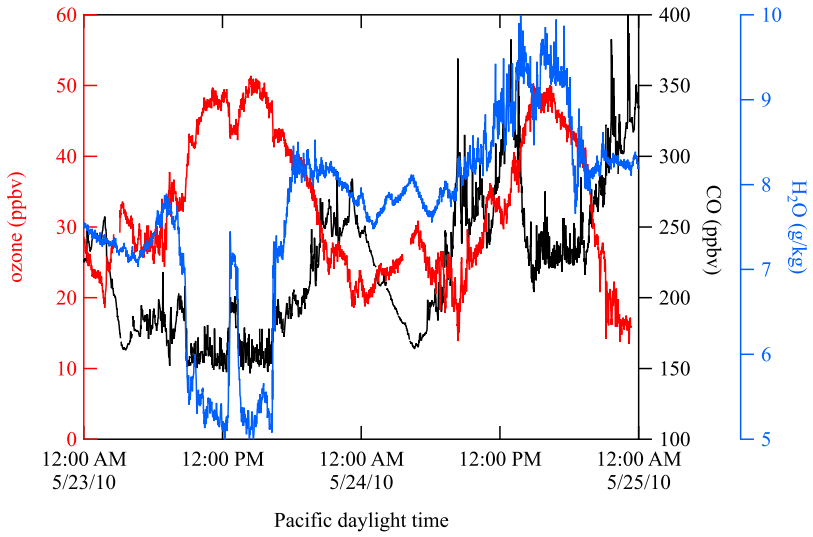

Figure 10. One-minute measurements of ozone (red), CO (black), and water vapor (blue) at the Pasadena, CA ground site.

model. Large differences between measured and modeled CO in the LA basin PBL suggest that ozone sources to the LA basin could not be identified and quantified using FLEXPART.

4.3. FT Air Mixes to the LA Basin Surface

[30] Ozone in the FT is of immediate importance to human health and vegetation only if it reaches the surface. Ozone in the FT over the LA basin was regularly near or above 75 ppbv (Figure 3), and correlations of ozone with CO and HNO_3 (Figures 7 and 8) demonstrate that FT air was entrained into the LA basin PBL. Usually, entrainment of FT air into the PBL occurred gradually as the PBL height slowly grew throughout the day. The PBL height averaged 1 km during this study, and it was higher later in the day. For example, the PBL over Redlands on 8 May grew from 1.2 km AGL at 1 P.M. PDT to 1.8 km AGL at 3:20 P.M. PDT (Figure 4). The PBL also deepened as air from the Pacific Ocean traveled inland and warmed as it traversed the LA basin. Dilution caused by gradual entrainment of air at the top of a growing PBL followed by mixing throughout the depth of the boundary layer can obscure the signatures of FT air at the surface. The frequency and extent of this downward mixing from the FT to the surface in California is examined in the work of *Langford et al.* [2012].

[31] On occasion, FT air mixed into the PBL so rapidly that the fingerprint of the FT was clearly evident at the surface. During the CalNex study, extensive chemical and meteorological measurements were made at a ground site in Pasadena from mid-May to mid-June. The smallest water vapor and daytime CO at the CalNex Pasadena ground site were recorded on 23 May (Figure 10) and were anti-correlated with ozone. The ozone mixing ratios on 23 May were similar to those measured one day earlier (not shown) and later, but the increased ozone and decreased CO and water vapor indicates that ozone on 23 May came from downward mixing of air with UT characteristics. Strong mixing of air from aloft to the surface in the LA basin usually reduced surface levels of CO and other trace gases, but ozone did not necessarily decrease.

4.4. FT Air Mixes Into the San Joaquin Valley PBL

[32] Downward mixing of ozone from the FT also was observed outside the LA basin. For example, on 18 June the WP-3D aircraft encountered dry air in the San Joaquin Valley PBL. Figure 11 shows ozone, water vapor, and CO measured from west to east across the San Joaquin Valley over agricultural land south of Merced, CA. On four vertical profiles performed near this flight segment, the PBL height was greater than 0.9 km AGL. Hence, these measurements at 0.4 km AGL were well within the PBL. Throughout this flight leg, NO_2 was less than 2 ppbv and the effects of ozone titration were inconsequential, so ozone rather than Ox is shown. On the west side of the San Joaquin Valley, CO and HNO_3 (not shown) were small, and ozone and water vapor were anti-correlated, indicating that UT air mixed into the PBL. Ozone increased more than 15 ppbv when this dry air from the FT mixed down to the San Joaquin Valley. Similar ozone enhancements, but with a different source, were observed in aged regional pollution at the eastern end of the valley (−120° longitude in Figure 11), where HNO_3 and CO were enhanced and positively correlated with ozone.

4.5. FT Air Mixes Into the High Desert PBL

[33] Ozone levels are frequently increased in the high desert east of the LA basin. For example, at Joshua Tree National Park (elevation 1.24 km, 180 km east of Los Angeles shown in Figure 1), the daily maximum 8-h average ozone exceeded the 75 ppbv NAAQS threshold 53 times in 2010 (http://www.arb.ca.gov/aqmis2/ozone_annual.php). The high desert is regularly affected by emissions transported from the LA basin by westerly winds. But topography also makes this region susceptible to ozone exposure from the FT. Downwind of the San Bernardino and San Gabriel mountains, which have summits over 3 km that are regularly exposed to the FT, the formation of atmospheric rotors can enhance mixing between the FT and PBL [*Wallace and*

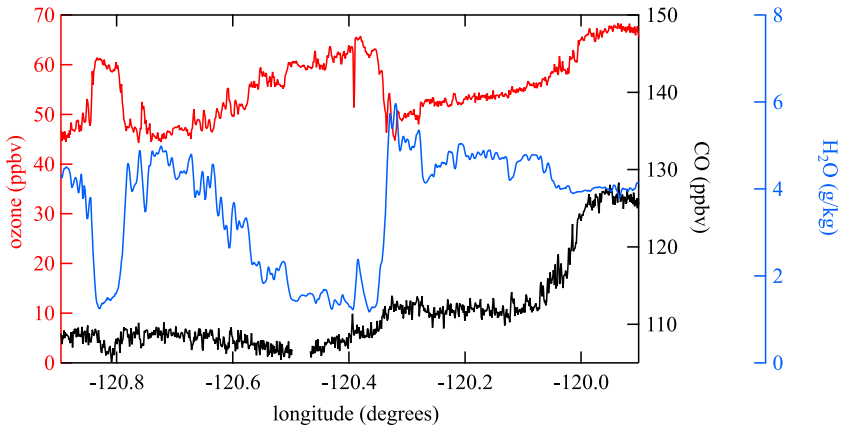

Figure 11. One-second measurements of ozone (red), CO (black), and water vapor (blue) on 18 June 2010, during a 95 km long flight leg at 0.4 km AGL over the San Joaquin Valley. The flight leg was conducted from 4:16–4:30 P.M. PDT at 36.9°–37.3° latitude. Winds were from the west at 8 m/s.

Hobbs, 1977]. Additionally, the high elevation and deep boundary layers in the high desert enhance exposure to FT air. Figure 12 shows a vertical profile over Joshua Tree National Park (Joshua Tree NP). In the PBL (<3 km), increased NOx (0.3–0.8 ppbv), HNO_3 (1–2.5 ppbv), and CO (120–143 ppbv) indicate that urban emissions were transported to this remote desert location. Just above the PBL, UT influences were evident, with decreased NOx (<0.2 ppbv) and HNO_3 (<0.5 ppbv), and ozone (>85 ppbv) was negatively correlated with CO. Deep boundary layers were observed regularly over the desert. For example, on 16 May, a vertical profile conducted over the same location later in the day (5:45 P.M. PDT) showed that the PBL had grown to 4 km altitude. Elevated PBL heights increase the high desert ozone concentrations by entraining ozone aloft.

[34] This mixing of FT air to the high desert may help explain the seasonal variability of ozone at Joshua Tree NP. Hourly ozone data are reported by the California Air Resources Board (www.arb.ca.gov/aqmis2/ozone_ytd.php) and include National Park Service measurements from Joshua Tree NP and South Coast Air Quality Management District measurements from Redlands. Figure 13 shows the number of days in each month (2006–2010 average) that daily maximum 8-h average ozone exceeded 75 ppbv at Joshua Tree NP and Redlands. Both areas experienced approximately the same number of exceedances of the 8-h average ozone standard (62/yr at Joshua Tree NP and 66/yr at Redlands), but ozone was enhanced earlier in the year at Joshua Tree NP compared to Redlands. Transport of springtime ozone-rich FT air [*Oltmans and Levy*, 1994] into the high desert may contribute to ozone exceedances at Joshua Tree NP.

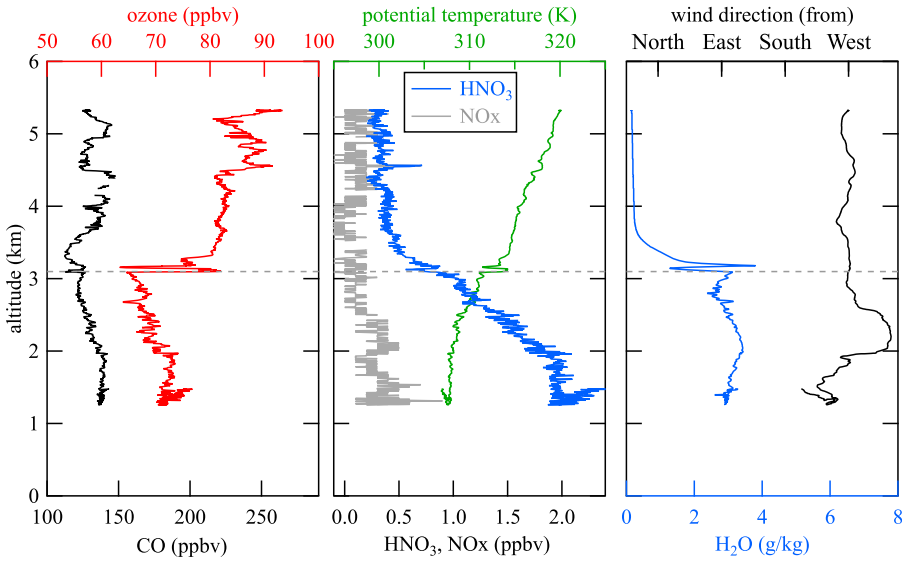

Figure 12. Same as Figure 4 but for a profile over Joshua Tree NP at 3:15 P.M. PDT on 4 May 2010. Since CLD instrument diagnostics were performed during this ascent, NOx data from the cavity ring-down spectrometer are shown.

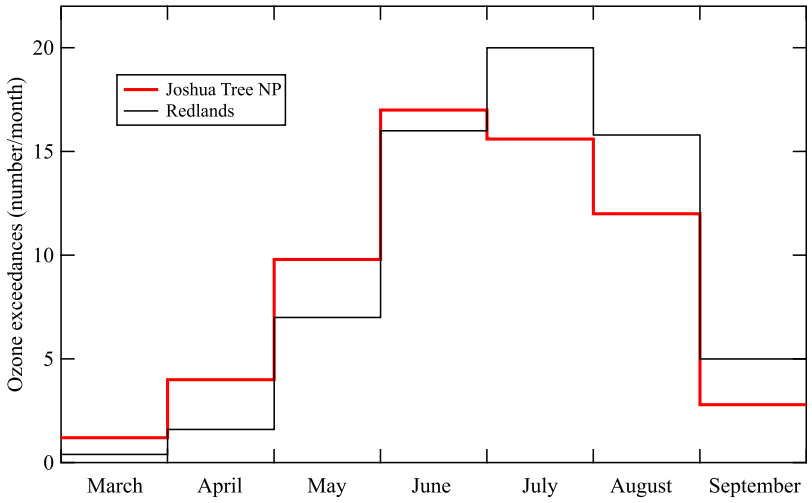

Figure 13. Number of days each month with daily maximum 8-h average ozone greater than 75 ppbv at Joshua Tree NP (red) and Redlands (black), averaged from 2006–2010.

4.6. Comparisons With Previous Studies

[35] Previous measurement campaigns observed air masses with similar characteristics and ozone levels just above the PBL over the LA basin. In 2002, during the International Transport and Chemical Transformation (ITCT) study [e.g., *Neuman et al.*, 2003a; *Nowak et al.*, 2004], trace gases were measured in aircraft vertical profiles over Catalina Island, Redlands, and the Mojave Desert. Although only a few profiles were performed, increased ozone from several sources was observed. Ozone was greater than 65 ppbv in the FT just above the PBL over the LA basin on 13 May 2002 and over the Mojave on 25 April 2002. The chemical composition of these air masses showed influences from dry UT air, long-range transport of emissions, and aged regional emissions.

[36] Measurements aboard commercial aircraft that arrived and departed from Los Angeles International Airport demonstrate that the observations reported here are regular features of the atmosphere over the LA Basin. The same region and season were sampled in May and June 2005 by the Measurement of ozone and water vapor by Airbus in-service aircraft program (MOZAIC) [*Marenco et al.*, 1998], which reported ozone and water vapor on eight departures and eight arrivals each month (http://mozaic.aero.obs-mip.fr/web/). Layers with increased ozone and decreased water vapor, characteristic of air descended from the UT, were observed regularly in the FT above LA. As an example, ozone, water vapor, and temperature are shown in Figure 14 for the afternoon departure on 7 June 2005. During the ascent, the aircraft traveled west from Los Angeles over the Pacific Ocean. The top of the PBL is indicated by the

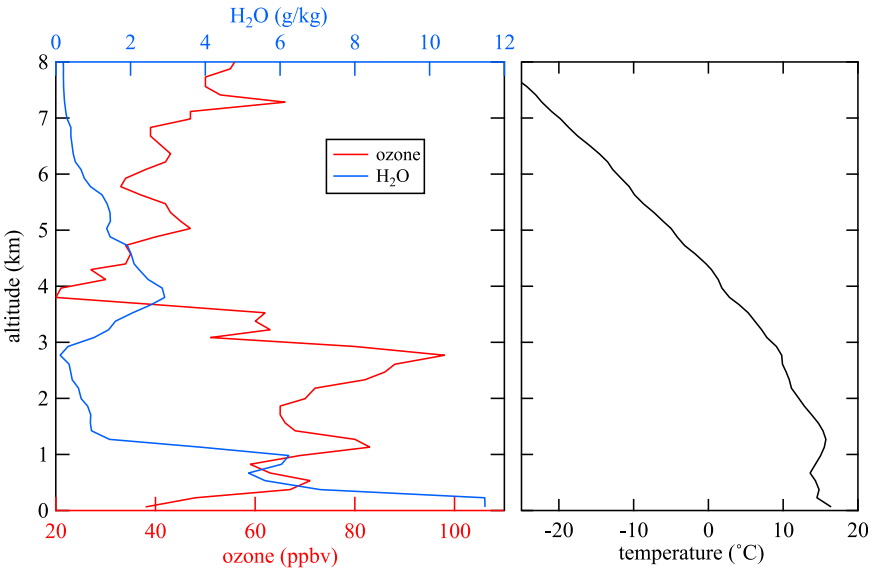

Figure 14. MOZAIC measurements of ozone (red), water vapor (blue), and temperature (black) over the LA Basin and Pacific Ocean following a 4:30 P.M. PDT departure from Los Angeles, CA on 7 June 2005.

temperature inversion at approximately 1 km altitude. Just above the PBL from 1–3 km, the air was dry and O_3 > 80 ppbv, similar to the UT air masses shown in section 3. Similar results were obtained during the aircraft arrival from the east that occurred 2 h earlier, and also over Portland, Oregon and San Francisco, CA, showing that this UT influence was persistent and not limited to the LA basin.

[37] Layers with increased water vapor and decreased ozone (e.g., from 3–5 km in Figure 14), likely resulting from transport of air from the marine boundary layer, were also encountered in the FT over the west coast of the U.S. Layers with either marine or UT influences were at different altitudes on different days. Consequently, ozone averaged over many vertical profiles from several years and locations does not exhibit a clear signature of UT influence [*Pfister et al.*, 2011, Figure 9]. However, the large ozone variability in the lower FT over the western U.S. (standard deviations of nearly 20 ppbv [*Pfister et al.*, 2011]) reflects the influence of sources with greatly differing ozone mixing ratios.

5. Summary

[38] In the lower FT over the LA basin, ozone mixing ratios were often large and equivalent to those in the highly polluted eastern LA basin PBL. Ozone in the FT had several sources, and downward mixing of ozone from the FT to the PBL over southern California increased ozone levels at the surface.

[39] Analysis of airborne in situ measurements of CO, reactive nitrogen, and water vapor in vertical profiles from 0.2–3.5 km AGL on six flights of the NOAA WP-3D aircraft over and adjacent to the LA basin were used to identify four distinct air mass types in the FT over the LA basin. Ozone averaged over 65 ppbv in three different air mass types that accounted for 89% of the observations measured in the FT during vertical profiles. Westerly winds, decreased CO, NOx, HNO_3, and water vapor, and backward trajectories from the Pacific Ocean often characterized the FT over the LA basin. In these cases, downward mixing from the UT resulted in ozone of 71 $\pm$ 8 ppbv in the FT between 1.8–3.5 km AGL. UT influenced air masses were the most frequently encountered air mass type in the FT over the LA basin. In air masses influenced by long-range transport of emissions, ozone mixing ratios were similar to those in UT air. On three flights, aged regional emissions were encountered in the FT over the LA basin. Winds with southerly and easterly components and increased HNO_3, CO, and water vapor indicated that the air had a continental source, and small NOx values established that the emissions were aged. In these air masses, ozone mixing ratios were less (65 $\pm$ 4 ppbv) than in the dry air masses. Less frequently, the FT was influenced by marine air with relatively decreased ozone (53 $\pm$ 10 ppbv). Ozone averaged 67 ppbv in the FT from 1.8–3.5 km, with similar mixing ratios in air masses influenced by the UT, aged regional emissions, and long-range transport of emissions.

[40] Correlations of ozone with CO and with NOx oxidation products demonstrate that ozone from the FT mixed into the PBL over the LA basin, high desert, and San Joaquin Valley. This ozone contribution from the FT is important to air quality policy, since the air just above the PBL over the LA basin had ozone mixing ratios near or greater than 75-ppbv, which is the daily maximum 8-h average U.S. standard.

[41] **Acknowledgments.** We thank the NOAA WP-3D flight and support crew for their efforts in achieving the flights in the LA Basin. The original ERA-interim data are available from the Research Data Archive at NCAR (http://dss.ucar.edu) in data set ds627.0.

References

Ambrose, J. L., D. R. Reidmiller, and D. A. Jaffe (2011), Causes of high O_3 in the lower free troposphere over the Pacific Northwest as observed at the Mt. Bachelor Observatory, *Atmos. Environ.*, *45*, 5302–5315, doi:10.1016/j.atmosenv.2011.06.056.

Blumenthal, D. L., W. H. White, and T. B. Smith (1978), Anatomy of a Los Angeles smog episode: Pollutant transport in the daytime sea breeze regime, *Atmos. Environ.*, *12*, 893–907, doi:10.1016/0004-6981(78)90028-8.

Chin, M., D. J. Jacob, J. W. Munger, D. D. Parrish, and B. G. Doddridge (1994), Relationship of ozone and carbon monoxide over North America, *J. Geophys. Res.*, *99*, 14,565–14,573, doi:10.1029/94JD00907.

Cooper, O. R., et al. (2010), Increasing springtime ozone mixing ratios in the free troposphere over western North America, *Nature*, *463*(7279), 344–348, doi:10.1038/nature08708.

Cooper, O. R., et al. (2011), Measurement of western U.S. baseline ozone from the surface to the tropopause and assessment of downwind impact regions, *J. Geophys. Res.*, *116*, D00V03, doi:10.1029/2011JD016095.

Croes, B. E., and E. M. Fujita (2003), Overview of the 1997 southern California ozone study (SCOS97-NARSTO), *Atmos. Environ.*, *37*, 3–26, doi:10.1016/S1352-2310(03)00379-0.

Edinger, J. G. (1973), Vertical distribution of photochemical smog in Los Angeles basin, *Environ. Sci. Technol.*, *7*, 247–252, doi:10.1021/es60075a004.

Fast, J. D., J. C. Doran, W. J. Shaw, R. L. Coulter, and T. J. Martin (2000), The evolution of the boundary layer and its effect on air chemistry in the Phoenix area, *J. Geophys. Res.*, *105*(D18), 22,833–22,848, doi:10.1029/2000JD900289.

Fiore, A. M., D. J. Jacob, I. Bey, R. M. Yantosca, B. D. Field, A. C. Fusco, and J. G. Wilkinson (2002), Background ozone over the United States in summer: Origin, trend, and contribution to pollution episodes, *J. Geophys. Res.*, *107*(D15), 4275, doi:10.1029/2001JD000982.

Haagen-Smit, A. J. (1952), Chemistry and physiology of Los Angeles smog, *Ind. Eng. Chem.*, *44*, 1342–1346, doi:10.1021/ie50510a045.

Hacker, J. P., I. G. McKendry, and R. B. Stull (2001), Modeled downward transport of a passive tracer over western North America during an Asian dust event in April 1998, *J. Appl. Meteorol.*, *40*(9), 1617–1628, doi:10.1175/1520-0450(2001)040<1617:MDTOAP>2.0.CO;2.

Holloway, J. S., R. O. Jakoubek, D. D. Parrish, C. Gerbig, A. Volz-Thomas, S. Schmitgen, A. Fried, B. Wert, B. Henry, and J. R. Drummond (2000), Airborne intercomparison of vacuum ultraviolet fluorescence and tunable diode laser absorption measurements of tropospheric carbon monoxide, *J. Geophys. Res.*, *105*, 24,251–24,261, doi:10.1029/2000JD900237.

Huang, M., et al. (2010), Impacts of transported background ozone on California air quality during the ARCTAS-CARB period; a multi-scale modeling study, *Atmos. Chem. Phys.*, *10*(14), 6947–6968, doi:10.5194/acp-10-6947-2010.

Hudman, R. C., et al. (2004), Ozone production in transpacific Asian pollution plumes and implications for ozone air quality in California, *J. Geophys. Res.*, *109*, D23S10, doi:10.1029/2004JD004974.

Jacob, D. J., J. A. Logan, and P. P. Murti (1999), Effect of rising Asian emissions on surface ozone in the United States, *Geophys. Res. Lett.*, *26*, 2175–2178, doi:10.1029/1999GL900450.

Jaffe, D. (2011), Relationship between surface and free tropospheric ozone in the western U. S., *Environ. Sci. Technol.*, *45*, 432–438, doi:10.1021/es1028102.

Langford, A. O., C. J. Senff, R. J. Alvarez II, R. M. Banta, and R. M. Hardesty (2010), Long-range transport of ozone from the Los Angeles basin: A case study, *Geophys. Res. Lett.*, *37*, L06807, doi:10.1029/2010GL042507.

Langford, A. O., J. Brioude, O. R. Cooper, C. J. Senff, R. J. Alvarez II, R. M. Hardesty, B. J. Johnson, and S. J. Oltmans (2012), Stratospheric influence on surface ozone in the Los Angeles area during late spring and early summer of 2010, *J. Geophys. Res.*, *117*, D00V06, doi:10.1029/2011JD016766.

Lawson, D. R. (1990), The southern California air quality study, *J. Air Waste Manage. Assoc.*, *40*, 156–165.

Liang, Q., et al. (2007), Summertime influence of Asian pollution in the free troposphere over North America, *J. Geophys. Res.*, *112*, D12S11, doi:10.1029/2006JD007919.

Lu, R., and R. P. Turco (1996), Ozone distributions over the Los Angeles Basin: Three-dimensional simulations with the SMOG model, *Atmos. Environ.*, *30*, 4155–4176, doi:10.1016/1352-2310(96)00153-7.

Marenco, A., et al. (1998), Measurement of ozone and water vapor by Airbus in-service aircraft: The MOZAIC airborne program, an overview, *J. Geophys. Res.*, *103*, 25,631–25,642, doi:10.1029/98JD00977.

McDonald-Buller, E. C., et al. (2011), Establishing policy relevant background (PRB) ozone concentrations in the United States, *Environ. Sci. Technol.*, *45*, 9484–9497, doi:10.1021/es2022818.

McElroy, J. L., and T. B. Smith (1993), Creation and fate of ozone layers aloft in southern California, *Atmos. Environ., Part A*, *27*, 1917–1929.

McKendry, I. G., J. P. Hacker, R. B. Stull, S. Sakiyam, D. Mignacca, and K. Reid (2001), Long-range transport of Asian dust to the Lower Fraser Valley, British Columbia, Canada, *J. Geophys. Res.*, *106*(D16), 18,361–18,370, doi:10.1029/2000JD900359.

Neuman, J. A., L. G. Huey, T. B. Ryerson, and D. W. Fahey (1999), Study of inlet materials for sampling atmospheric nitric acid, *Environ. Sci. Technol.*, *33*, 1133–1136, doi:10.1021/es980767f.

Neuman, J. A., et al. (2001), In situ measurements of HNO_3, NO_y, NO, and O_3 in the lower stratosphere and upper troposphere, *Atmos. Environ.*, *35*, 5789–5797, doi:10.1016/S1352-2310(01)00354-5.

Neuman, J. A., et al. (2002), Fast-response airborne in situ measurements of HNO_3 during the Texas Air Quality Study, *J. Geophys. Res.*, *107*(D20), 4436, doi:10.1029/2001JD001437.

Neuman, J. A., et al. (2003a), Variability in ammonium nitrate formation and nitric acid depletion with altitude and location over California, *J. Geophys. Res.*, *108*(D17), 4557, doi:10.1029/2003JD003616.

Neuman, J. A., T. B. Ryerson, L. G. Huey, R. Jakoubek, J. B. Nowak, C. Simons, and F. C. Fehsenfeld (2003b), Calibration and evaluation of nitric acid and ammonia permeation tubes by UV optical absorption, *Environ. Sci. Technol.*, *37*, 2975–2981, doi:10.1021/es026422l.

Neuman, J. A., et al. (2009), Relationship between photochemical ozone production and NO_x oxidation in Houston, Texas, *J. Geophys. Res.*, *114*, D00F08, doi:10.1029/2008JD011688.

Nowak, J. B., et al. (2004), Gas-phase chemical characteristics of Asian emission plumes observed during ITCT 2K2 over the eastern North Pacific Ocean America, *J. Geophys. Res.*, *109*, D23S19, doi:10.1029/2003JD004488.

Nowak, J. B., J. A. Neuman, K. Kozai, L. G. Huey, D. J. Tanner, J. S. Holloway, T. B. Ryerson, G. J. Frost, S. A. McKeen, and F. C. Fehsenfeld (2007), A chemical ionization mass spectrometry technique for airborne measurements of ammonia, *J. Geophys. Res.*, *112*, D10S02, doi:10.1029/2006JD007589.

Oltmans, S. J., and H. Levy II (1994), Surface ozone measurements from a global network, *Atmos. Environ.*, *28*, 9–24, doi:10.1016/1352-2310(94)90019-1.

Parrish, D. D., M. Trainer, J. S. Holloway, J. E. Yee, M. S. Warshawsky, F. C. Fehsenfeld, G. L. Forbes, and J. L. Moody (1998), Relationships between ozone and carbon monoxide at surface sites in the North Atlantic Region, *J. Geophys. Res.*, *103*(D11), 13,357–13,376, doi:10.1029/98JD00376.

Parrish, D. D., et al. (2004), Changes in the photochemical environment of the temperate North Pacific troposphere in response to increased Asian emissions, *J. Geophys. Res.*, *109*, D23S18, doi:10.1029/2004JD004978.

Parrish, D. D., K. C. Aikin, S. J. Oltmans, B. J. Johnson, M. Ives, and C. Sweeny (2010), Impact of transported background ozone inflow on summertime air quality in a California ozone exceedance area, *Atmos. Chem. Phys.*, *10*, 10,093–10,109, doi:10.5194/acp-10-10093-2010.

Pfister, G., et al. (2011), Characterizing summertime chemical boundary conditions for airmasses entering the US West Coast, *Atmos. Chem. Phys.*, *11*, 1769–1790, doi:10.5194/acp-11-1769-2011.

Pollack, I. B., B. M. Lerner, and T. B. Ryerson (2011), Evaluation of ultraviolet light-emitting diodes for detection of atmospheric NO_2 by photolysis - chemiluminescence, *J. Atmos. Chem.*, *65*(2), 111–125, doi:10.1007/s10874-011-09184-3.

Popp, P. J., et al. (2009), Stratospheric correlation between nitric acid and ozone, *J. Geophys. Res.*, *114*, D03305, doi:10.1029/2008JD010875.

Roberts, J. M., et al. (2004), Measurement of peroxycarboxylic nitric anhydrides (PANs) during the ITCT 2K2 aircraft intensive experiment, *J. Geophys. Res.*, *109*, D23S21, doi:10.1029/2004JD004960.

Ryerson, T. B., et al. (1998), Emissions lifetimes and ozone formation in power plant plumes, *J. Geophys. Res.*, *103*(D17), 22,569–22,583, doi:10.1029/98JD01620.

Simmons, A., S. Uppala, D. Dee, and S. Kobayashi (2007), ERA-Interim: New ECMWF reanalysis products from 1989 onwards, *ECMWF Newsl.*, *110*, 11 pp.

Slusher, D. L., L. G. Huey, D. J. Tanner, F. M. Flocke, and J. M. Roberts (2004), A thermal dissociation-chemical ionization mass spectrometry (TD-CIMS) technique for the simultaneous measurement of peroxyacylnitrates and dinitrogen pentoxide, *J. Geophys. Res.*, *109*, D19315, doi:10.1029/2004JD004670.

Stohl, A., C. Forster, A. Frank, P. Seibert, and G. Wotawa (2005), Technical note: The Lagrangian particle dispersion model FLEXPART version 6.2, *Atmos. Chem. Phys.*, *5*, 2461–2474, doi:10.5194/acp-5-2461-2005.

Trainer, M., et al. (1993), Correlation of ozone with NO_y in photochemically aged air, *J. Geophys. Res.*, *98*, 2917–2925, doi:10.1029/92JD01910.

Trickl, T., N. Bartsch-Ritter, H. Eisele, M. Furger, R. Mucke, M. Sprenger, and A. Stohl (2011), High-ozone layers in the middle and upper troposphere above Central Europe: Potential import from the stratosphere along the subtropical jet stream, *Atmos. Chem. Phys.*, *11*, 9343–9366, doi:10.5194/acp-11-9343-2011.

Wagner, N. L., W. P. Dubé, R. A. Washenfelder, C. J. Young, I. B. Pollack, T. B. Ryerson, and S. S. Brown (2011), Diode laser-based cavity ring-down instrument for NO_3, N_2O_5, NO, NO_2 and O_3 from aircraft, *Atmos. Meas. Tech.*, *4*, 1227–1240, doi:10.5194/amt-4-1227-2011.

Wallace, J. M., and P. V. Hobbs (1977), Clouds and storms, in *Atmospheric Science: An Introductory Survey*, pp. 215–278, Academic, San Diego, Calif.

Wang, H., D. J. Jacob, P. Le Sager, D. G. Streets, R. J. Park, A. B. Gilliland, and A. van Donkelaar (2009), Surface ozone background in the United States: Canadian and Mexican pollution influences, *Atmos. Environ.*, *43*, 1310–1319, doi:10.1016/j.atmosenv.2008.11.036.

Zhang, L., et al. (2008), Transpacific transport of ozone pollution and the effect of recent Asian emission increases on air quality in North America: An integrated analysis using satellite, aircraft, ozonesonde, and surface observations, *Atmos. Chem. Phys.*, *8*, 6117–6136, doi:10.5194/acp-8-6117-2008.

Zhang, L., et al. (2011), Improved estimate of the policy-relevant background ozone in the United States using the GEOS-Chem global model with 1/2°×2/3° horizontal resolution over North America, *Atmos. Environ.*, *45*, 6769–6776, doi:10.1016/j.atmosenv.2011.07.054.

K. C. Aikin, W. M. Angevine, S. S. Brown, J. A. de Gouw, W. P. Dube, M. Graus, J. S. Holloway, J. B. Nowak, D. D. Parrish, I. B. Pollack, J. M. Roberts, T. B. Ryerson, M. Trainer, and N. L. Wagner, Chemical Sciences Division, Earth System Research Laboratory, NOAA, 325 Broadway, Boulder, CO 80305, USA.

J. Brioude and J. A. Neuman, Cooperative Institute for Research in Environmental Sciences, University of Colorado Boulder, R/CSD 7, 325 Broadway, Boulder, CO 80305, USA. (andy.neuman@noaa.gov)

J. H. Flynn and B. L. Lefer, Department of Earth and Atmospheric Sciences, University of Houston, Houston, TX 77204, USA.

P. Nedelec and V. Thouret, Laboratoire d'Aérologie, Centre National de la Recherche Scientifique, 14 Av. E. Belin, F-31400 Toulouse, France.

H. Smit, Institute for Chemistry of the Polluted Atmosphere, Research Centre Jülich GmbH, PO Box 1913, D-52425 Jülich, Germany.